Macrocyclic copper(II) complexes containing diazacyclam-based ligand: Spectral, structuraland docking studies

Zahra Mardani*[a], Keyvan Moeini[b], Majid Darroudi[c], Cameron Carpenter-Warren[d], Alexandra M. Z. Slawin[d] and J. Derek Woollins[d]

[a]Inorganic Chemistry Department, Faculty of Chemistry, Urmia University, 57561-51818 Urmia, I. R. Iran

[b]Chemistry Department, Payame Noor University, 19395-4697 Tehran, I. R. Iran

[c]Nuclear Medicine Research Center, Mashhad University of Medical Sciences, Mashhad, I. R. Iran

[d]EaStCHEM School of Chemistry, University of St Andrews, St Andrews Fife UK, KY16 9ST

*Corresponding author:
Zahra Mardani
E-mail: z.mardani@urmia.ac.ir
Fax: +98 4432752746

ABSTRACT

The macrocyclic copper complex, [Cu(ACE)(NO_3)$_2$]; ACE: 1,3,6,10,12,15-hexaazatricyclo[13.3.1.1^{6,10}]eicosane, was synthesized by template condensation from a mixture of N^1-(2-aminoethyl)-1,3-diaminopropane, formaldehyde and copper(II) nitrate. Replacement of the nitrate with thiocyanato and azido ligands gives [Cu(ACE)NSC]NSC (**2**) and the 1D-coordination polymer, [Cu(ACE)(μ-N_3)]$_n$[N_3]$_n$ (**3**), respectively. Complex **1**, [Cu(ACE)(NO_3)]NO_3, is an intermediate product in which one of the nitrate ions is separated from its parent molecule. Formation of **1** allow us to conclude that the mechanism of ion exchange reactions on its parent molecule is similar to SN1. These complexes have been characterized by FT-IR spectroscopy and X-ray crystallography. In the crystal structures of **1** and **2**, the copper(II) ion has a distorted square pyramidal geometry in which the N_4-donor ACE ligand lies on the equatorial plane and other ligand occupies the axial position. The copper(II) ion in **3** has an octahedral geometry, coordinating to one ACE ligand in the equatorial plane and two N-donor bridging azido groups in the axial positions. In all structures, owing to the Jahn-Teller effect, the coordinated bond length of the axial position is longer than the equatorial ones. The ability of ACE ligand and its complexes **1** and **2**, along with their analogues, to interact with ten selected biomacromolecules (BRAF kinase, CatB, DNA gyrase, HDAC7, rHA, RNR, TrxR, TS, Top II, B-DNA) was investigated by docking calculations and compared with that of doxorubicin.

Keywords: Macrocycle; Diazacyclam; Copper complex; Template synthesis; Docking study

1. Introduction

Macrocycles are an important class of ligands in transition metal chemistry since they can provide beneficial thermodynamic and kinetic properties to their metal complexes [1-4] and increase the ability of coordinated metals to access their less common oxidation states [5]. There are a board range of applications for these types of ligands and their complexes, such as sensors [6, 7], metal ion-selective reagents [8], nitric oxide [9, 10] and superoxide anion [11] scavengers, precursors for luminescent compound formation, MRI contrast agents and radiopharmaceuticals [12]. Macrocyclic copper complexes can participate in ion exchange reactions [13-15] and also form coordination polymers [14].

With regard to medicinal applications, they are used in the modelling of metallobiosites [16] and metalloenzyme active sites [17] and also have also shown anti-AIDS/HIV [11, 18], anti-fertility, anti-bacterial, anti-fungal [19], anti-microbial and anti-oxidant [20] activities. The use of pentaazamacrocyclic manganese(II) compounds as superoxide dismutase (SOD) mimetics has been further investigated [21]. Macrocyclic copper(II) complexes have been found to react with DNA by different binding modes and to exhibit effective nuclease activity [22-25].

In the field of catalytic applications, transition metal macrocyclic complexes have shown excellent catalytic properties for many inner-sphere electrochemical reactions [7, 26, 27]. MN_4 macrocyclic complexes are one special class of non-precious metal catalysts (NPMC) [28]. They are used as new catalysts in modern synthetic organic chemistry [29, 30] and also effective catalysts in asymmetric synthesis [31]. Study of the literature revealed that there are various reactions for the synthesis of the macrocyclic compounds including those which form C–C, C–O, C–S, C–N, C=N and B–O bonds [15].

In the following, we report the synthesis and characterization (FT-IR, X-ray) of two new copper(II) macrocyclic complexes, $[Cu(ACE)NO_3]NO_3$ (**1**) and [Cu(ACE)NCS]NCS (**2**), containing the macrocyclic ligand 1,3,6,10,12,15-hexaazatricyclo[13.3.1.$1^{6,10}$]eicosane (ACE, Scheme 1) along with a macrocyclic 1D-coordination polymer, $[Cu(ACE)(\mu\text{-}N_3)]_n[N_3]_n$ (**3**). These compounds were prepared by template condensation and then ion exchange reactions.

The expected biological properties of macrocyclic copper complexes [22-25] make them good candidates as biologically active compounds, thus docking calculations were run to investigate the possibility of interactions between the ACE ligand, its complexes (**1** and **2**) and their analogues with ten biomacromolecule targets [32-34], including: BRAF kinase, Cathepsin B (CatB), DNA gyrase, Histone deacetylase (HDAC7), recombinant Human albumin (rHA), Ribonucleotide reductases (RNR), Thioredoxin reductase (TrxR), Thymidylate synthase (TS), Topoisomerase II (Top II) along with B-DNA. These proteins were selected either due to their reported roles in cancer growth or as transport agents that affect drug pharmacokinetic properties (e.g., rHA). The DNA gyrase was included to study the possibility of anticancer properties and their activity as antimalarial agents [35]. The knowledge gained from docking on the B-DNA should be useful for the development of potential probes for DNA structure and new therapeutic reagents for tumors and other diseases [36].

2. Experimental

2.1. Instrumentation and reagents

All starting chemicals and solvents were purchased from Sigma Aldrich with reagent or analytical grade and used as received. The $[Cu(ACE)(NO_3)_2]$ precursor was synthesized according to the our previous report [15]. The carbon, hydrogen and nitrogen contents were

determined using a Thermo Finnigan Flash Elemental Analyzer 1112 EA. The infrared spectra of a KBr pellets were recorded in the range 4000–400 cm^{-1} using a FT-IR 8400-Shimadzu spectrometer. Melting points were determined using a Barnsted Electrothermal 9200 electrically heated apparatus.

2.1.1. Synthesis of 1,3,6,10,12,15-hexaazatricyclo[13.3.1.1^{6,10}]eicosanenitratocopper(II) nitrate, [Cu(ACE)NO$_3$]NO$_3$, (1)

[Cu(ACE)$(NO_3)_2$] (0.40 g, 0.85 mmol) and $Zn(NO_3)_2 \cdot 6H_2O$ (0.25 g, 0.84 mmol) were placed in the large arms of a branched tube. Ethanol was carefully added to fill both arms. The tube was then sealed and the ligand-containing arm was immersed in a bath at 60 °C while the other was maintained at ambient temperature [32, 33, 37]. After a week, violet crystals deposited in the cooler arm were filtered off and dried in air. Yield (0.04 g) 10%; m.p. 199 °C. Anal. Calcd for $C_{14}H_{30}CuN_8O_6$ (%): C, 35.78; H, 6.43; N, 23.84. Found: C, 35.90; H, 6.51; N, 23.96. IR (KBr, cm^{-1}): 3269 m (ν N−H), 2935 m (ν_{as} CH_2), 2860 m (ν_s CH_2), 1465 m (δ_{as} CH_2), 1403 s (δ_s CH_2), 1360 s (ν_4 NO_3), 1320 s (ν_4 NO_3^{free}), 1268 m (ν_1 NO_3), 1086 m (ν_2 NO_3), 1046 m (ν C−N), 818 m (ν_6 NO_3).

Also in similar reaction, $Zn(NO_3)_2 \cdot 6H_2O$ was replaced by $NaNO_3$ (0.25 g, 0.07 mmol); in the cooler arm the non-ionic analogue of **1** (starting precursor) was crystallized (characterized by melting point, there is about 50 °C difference between melting point of **1** and analogue of **1** [15]). Yield (0.22 g) 55%; m.p. 245 °C.

2.1.2. Synthesis of 1,3,6,10,12,15-hexaazatricyclo[13.3.1.1^{6,10}]eicosanethiocyanatocopper(II) thiocyanate, [Cu(ACE)NCS]NCS, (2)

A solution of KSCN (0.15 g, 1.54 mmol), dissolved in H_2O (10 mL), was added to the solution of [Cu(ACE)$(NO_3)_2$] (0.36 g, 0.77 mmol) in H_2O (20 mL). The reaction mixture was stirred at 60 °C for 2 h. Purple crystals were obtained by slow evaporation of the solution and filtration (this product was reported in our previous work [13]). The filtered solution then gave rise to an oily product which was dissolved in the methanol. Aqua crystals of the product suitable for X-ray diffraction studies were obtained by slow evaporation of the solution. The crystals were then collected by filtration. Yield (0.03 g) 2%; m.p. 148 °C, decomposed. Anal. Calcd for $C_{64}H_{118}Cu_4N_{32}O_3S_8$ (%): C, 50.23; H, 7.77; N, 5.49. Found: C, 50.38; H, 7.79; N, 5.63. IR (KBr, cm^{-1}): 3439 m (ν O−H), 3130 m (ν N−H), 2951 m (ν_{as} CH_2), 2855 m (ν_s CH_2), 2061 s (ν CN^{NCS}), 1647 w (δ H_2O), 1455 m (δ_{as} CH_2), 1379 m (δ_s CH_2), 1064 m (ν C−N), 818 m (ν C–S), 624 w (ρ_r H_2O), 537 (ρ_w H_2O).

2.1.3. Synthesis of catena{1,3,6,10,12,15-hexaazatricyclo[13.3.1.1^{6,10}]eicosaneazidocopper(II)} azide, [Cu(ACE)(μ-N_3)]$_n$[N_3]$_n$ (3)

The procedure for synthesis of **3** was similar to **1**, except that the $Zn(NO_3)_2 \cdot 6H_2O$ was replaced by NaN_3 (0.11 g, 1.70 mmol) and ethanol with methanol. After a week, violet crystals deposited in the cooler arm were filtered off and dried in air. Yield (0.10 g) 27%; m.p. 185−190 °C. IR (KBr, cm^{-1}): 3236 m (ν N−H), 2945 m (ν_{as} CH_2), 2867 m (ν_s CH_2), 2039 s (ν_{as} NNN), 1467 m (δ_{as} CH_2), 1380 s (ν_4 NO_3), 1335 s (ν_s NNN), 1280 m (ν_1 NO_3), 1090 m (ν_2 NO_3), 1039 m (ν C−N), 810 m (ν_6 NO_3), 643 m (δ NNN).

2.2. Crystal structure determination and refinement

X-ray diffraction data for **1** was collected at 125 K using the St Andrews Automated Robotic Diffractometer (STANDARD) [38] consisting of a Rigaku sealed-tube generator, equipped with

a SHINE monochromator [Mo Kα radiation (λ = 0.71075 Å)], and a Saturn 724 CCD area detector, coupled with a Microglide goniometer head and an ACTOR SM robotic sample changer. The data for **2** was collected at 173 K by using a Rigaku FR-X Ultrahigh Brilliance Microfocus RA generator/confocal optics with XtaLAB P200 diffractometer [Mo Kα radiation (λ = 0.71075 Å)]. Data for **3** was collected at 125 K by using a Rigaku MM-007HF High Brilliance RA generator/confocal optics with XtaLAB P200 diffractometer [Cu Kα radiation (λ = 1.54187 Å)]. Intensity data for all samples was collected using ω steps accumulating area detector images spanning at least a hemisphere of reciprocal space. All data were corrected for Lorentz polarization effects. A multiscan absorption correction was applied by using CrystalClear [39] for **1** and CrysAlisPro [40] for **2** and **3**. All structures were solved using dual space methods (SHELXT [41]) and refined by full-matrix least-squares against F^2 (SHELXL-2013 [42]). Non-hydrogen atoms were refined anisotropically, and hydrogens bound to heteroatoms were refined isotropically via the electron density map and held in place by light distance restraints, with the exception of H44 which was refined geometrically using a riding model. All other hydrogen atoms were refined geometrically using a riding model. All calculations were performed using the Olex2 interface [43]. The structure of **3** was submitted to the SQUEEZE procedure [44], which found 44 electrons per unit cell, which is close to the 42 electrons that would account for the two missing N_3^- ions, in said unit cell, which are likely highly disordered in the wide channels running down the *a* axis. Selected crystallographic data are presented in Table 1. Diagrams of the molecular structure and unit cell were created using Ortep-III [45, 46] and Diamond [47]. Selected bond lengths and angles are displayed in Table 2 and hydrogen bond geometries in Table 3.

2.3. Docking details

The pdb files 4r5y, 3ai8, 5cdn, 3c0z, 2bx8, 1peo, 3qfa, 1njb, 4gfh, 1bna for the ten receptors, BRAF kinase, Cathepsin B (CatB), DNA gyrase, Histone deacetylase (HDAC7), recombinant Human albumin (rHA), Ribonucleotide reductases (RNR), Thioredoxin reductase (TrxR), Thymidylate synthase (TS), Topoisomerase II (Top II), B-DNA, respectively, used in this research were obtained from the Protein Data Bank (pdb) [48]. The full version of Genetic Optimization for Ligand Docking (GOLD) 5.5 [49] was used for the docking studies. The Hermes visualizer in the GOLD Suite was used to further prepare the ligands, complexes and the receptors for docking. The cif files of the complexes and the optimized structure of the ligand were used for the docking studies. The region of interest used for Gold docking was defined as all the protein residues within 6 Å of the reference ligand "A" that accompanied the downloaded protein. For B-DNA, the region of interest was defined on the DNA backbone within 10 Å of the O4, DT19 and O2, DT19 atoms for major and minor grooves, respectively. All free water molecules in the structure of the proteins were deleted before docking. Default values of all other parameters were used and the compounds were submitted to 10 genetic algorithm runs using the GOLDScore fitness function.

3. Results and Discussion

Template condensation involving amine and formaldehyde, then ion exchange reactions were employed for the synthesis of the compounds. In case of the complex **1**, we decided to examine possibility of reaction between side non-coordinated nitrogen atoms of the $[Cu(ACE)(NO_3)_2]$ with $Zn(NO_3)_2$ and also we have reported similar reaction with $HgCl_2$ [14]. We could not prepare the desired complex but **1** was formed. It seems that the $Zn(NO_3)_2$ facilities formation of the complex **1**. All complexes are air-stable, and soluble in water and DMSO.

3.1. Spectroscopic characterization

In all spectra, the frequencies above 3000 cm^{-1} reveal the amine moieties in these compounds. Two bands under 3000 cm^{-1} confirm the aliphatic properties of the macrocyclic ligand. Four bands in the IR spectrum of **1** at 1360, 1268, 1086 and 818 cm^{-1} can be assigned to vibrations of the coordinated nitrate groups (respectively the vibrations ν_4, ν_1, ν_2 and ν_6). The difference between the ν_4 and the ν_1 peak positions is 92 cm^{-1}, which is typical for monodentate nitrate (bidentate nitrate displays a much larger splitting) [14, 37, 50].

The presence of water in **2** affects the IR spectrum in three regions [51, 52] including, above 3300 cm^{-1} for asymmetric and symmetric OH stretches, 1647 cm^{-1} for H_2O bending and 200–600 cm^{-1} for "librational modes". These modes are due to rotational oscillations of the water molecules restricted by interactions with neighboring atoms and they are classified into three types (wagging (ρ_w), twisting (ρ_t) and rocking (ρ_r)) depending on the direction of the principal axis of rotation [14, 53]. Another interesting aspect of this spectrum is the vibrations corresponding to the thiocyanate group. These bands include the C≡N stretching band at 2061 cm^{-1} [54] and the C−S stretching band at 818 cm^{-1} [37]. These bands can be used to determine the coordination mode of the thiocyanato ligand in its various complexes [24, 54]. The thiocyanate ion can coordinate to metal centers as an N-donor, S-donor or bridging N,S-donor ligand. The C≡N stretching frequencies are generally lower in N-bonded complexes (near and above 2050 cm^{-1}) than in S-bonded (near 2100 cm^{-1}) and bridging ones (above 2100 cm^{-1}) [54]. Based on these rules, it can be deduced that the thiocyanate ions in **1** are coordinated to the copper(II) ion as N-donor ligands. In addition, the observed ν (C−S) band in the IR spectrum

(818 cm^{-1}) is in accord with a N-bonded thiocyanato ligand (the frequency for S-bonded ones is about 50−120 cm^{-1} lower than this value [54]).

In compound **3**, the occurrence of a strong band at 2039 cm^{-1} indicates the presence of azido groups (ν_{as} NNN). The symmetrical stretching and also deformation mode of the azido ligand is observed as bands at 1335 and 640 cm^{-1}, respectively. Also a strong band at 1380 cm^{-1} reveals the presence of the nitrate group, which based on the structural analysis was not bonded to copper(II) ion.

3.2. Description of the crystal structures

Previously, we classified the different derivatives of ACD-based macrocyclic ligands (the main and important moiety of the ACE ligand is ACD unit, Scheme 1) and compared their structural parameters with cyclam-based analogues [15]. In this survey, all complexes containing ACD-based (simplest analogue of ACE) ligands (Scheme 1) were analyzed using the CSD software [55] to determine the percentage of the different coordinated metals to this unit. The data revealed that nickel is the most common metal in these systems, followed by copper (Fig. 1), which may be attributed to the fact that the macrocyclic hole-size of ACD-based ligands is suitable for these ions. There are two different coordination modes for ACD-based ligands including N_4 and N_5-donor. The N_4-donor mode (N1, N5, N8 and N12, Scheme 1) by far the most common, with there being only one example of the N_5-donor mode [14].

In another survey, all macrocyclic complexes of ACE were investigated. This study revealed that there are nine compounds; six ACE/Cu examples [14, 15, 56] and three ACE/Ni ones [57-59]. In all complexes, the ACE ligand act as N_4-donor (N1, N5, N8 and N12, Scheme 1) except in one case [14] in which in addition to the four nitrogen atoms of ACE, one of the side nitrogen

atoms of the macrocyclic ligand (N3 or N10, Scheme 1) also participates in complexation reaction. In the structures containing octahedral or square planar geometry around metal atom, distance of the metal atom from a mean plane through four coordinated nitrogen atoms is 0.003 Å, confirming that the metal atom placed on the hole of macrocyclic ligand while in the square pyramidal geometry the distance of metal is increased from the nitrogen atoms plane (0.579 Å), revealing that the metal atom placed out of macrocyclic hole.

3.2.1. Crystal structure of [Cu(ACE)NO$_3$]NO$_3$ (1)

We have previously reported the structure of [Cu(ACE)(NO$_3$)$_2$] [15] and established its ion exchange ability. Our investigations revealed that the nitrate ions were weakly bound to the copper(II) ion and can be readily replaced by other ions [13-15]. In this work we report an intermediate product, proving that the nitrate ions can be separated from their parent molecule. Based on this observation, the mechanism of ion exchange reaction on parent molecule of [Cu(ACE)(NO$_3$)$_2$] could be SN1. X-ray analysis of **1** (Fig. 2) revealed an ionic compound of copper. In this structure, the copper(II) ion is coordinated to one oxygen atom of a nitrato ligand and one N$_4$-donor ACE ligand with an overall coordination number of five. A pentacoordinate geometry may adopt either a square pyramidal or a trigonal bipyramidal structure. To determine the geometry for such complexes, the formula proposed by Addison *et al.* [60, 61] was applied. The angular structural parameter (τ) value for **1** was calculated to be 0.37, indicating a distorted square pyramidal geometry around the copper(II) ion, which is the most common 5-coordinate geometry for a copper(II) ion in complexes such as these [34]. Comparing the axial and equatorial bond lengths confirms slight elongation along the *z*-axis (the axial Cu–O bond length is 0.249 Å longer than the equatorial Cu–N average), consistent with pseudo Jahn-teller distortions observed in other Cu(II) square pyramidal structures [34, 62]. Comparing the

geometrical parameters of **1** with its non-ionic analogue, containing an octahedrally coordinated copper(II) ion, [Cu(ACE)(NO_3)$_2$] [15], revealed that the Cu–N distance average (2.046 and 2.040 Å for **1** and its analogue, respectively) is similar, whilst the Cu–O distances of the analogue (2.673 Å) are much longer than in **1** (2.2985(2) Å). This shows that the elongation down the z-axis is far more dramatic in octahedral geometry than in square pyramidal geometry. A mean plane through the coordinated atoms of the ACE with copper(II) ion in **1** revealed that these atoms do not lie a plane (r.m.s. deviation of 0.2494(9) Å for N12 and an average of 0.2032(7) for the 5 atoms) while the equivalent atoms in [Cu(ACE)(NO_3)$_2$] lie in a plane with negligible deviation.

The macrocyclic ligand is tetradentate forming two five- and two six-membered chelate rings which alternate on the equatorial plane. The average of the N–Cu–N bonding angles in the six-membered chelate rings is 93.52º and 85.91º for the five-membered chelate rings, which are comparable values to the CSD average (93.86 and 85.50 º, respectively [13]). The 1,3-diazacyclohexane subunits are fused to each of the six-membered chelate rings and have a chair conformation. Comparing the 1,3-diazacyclohexane ring of **1** with its analogue, [Cu(ACE)(NO_3)$_2$], revealed that the ACE ligand in **1** is the rotational isomer of the previously reported structure. In **1**, both of the 6-membered rings point in the same direction, towards the coordinated NO_3 unit, whereas in the previous structure one points up and one down, one towards each coordinated NO_3 unit. Based on our previous work on ACE macrocycles [13-15, 24] and also the low yield obtained for **1**, we can conclude that the isomer of ACE in **1** is not common and is likely the kinetically favored product of a fast crystallization process, rather than the previously characterized thermodynamically favored product [13-15, 24]. The ligand itself has no chiral centers, however four new ones are formed upon metal coordination (N1, N5, N8

and N12). The two secondary amine groups have the same enantiomeric form, which is different than that of the tertiary ones. The crystals contain a racemic mixture of *R*,*S*,*R*,*S* and *S*,*R*,*S*,*R* isomers.

The nitrate group which acts as a monodendate ligand is slightly asymmetric (bond lengths range 1.233–1.254 Å and angles range 119.0–120.5°). The non-bonded nitrate ion is also slightly asymmetric (bond lengths range 1.226–1.248 Å and angles range 119.5–120.9°). In crystal structure of **1**, there are relatively strong [63] intermolecular N–H···O hydrogen bonds (Table 3).

3.2.2. Crystal structure of [Cu(ACE)NCS]NCS (2)

Previously we reported the structure of $[Cu(ACE)(NCS)_2]$ as the major product of the reaction between $[Cu(ACE)(NO_3)_2]$ and KSCN. In this work we introduce another low yield product of this reaction. In the asymmetric unit of **2** (Fig. 3), there are two independent ionic complexes, two free thiocyanate anions, one water molecule and half a methanol – disordered over an inversion center. In the two coordinated macrocycles the copper center bonds to two secondary and two tertiary amines on the macrocycle and one nitrogen atom on the thiocyanato ligand, with a coordination number of five and square pyramidal geometry (τ = 0.46 and 0.42 for Cu1 and Cu21). The axial Cu–N bond lengths are longer than the equatorial Cu–N average (0.034 and 0.073 Å longer for the molecules containing Cu1 and Cu21 respectively), showing that the *z*-axis elongation in **2** is lower than in **1**. This may be attributed to the fact that the geometry in **1** is closer to ideal square pyramidal than in **2**. Comparing the geometrical parameters of **2** with its non-ionic analogue, $[Cu(ACE)(NCS)_2]$ [13], revealed that the $Cu–N^{ACE}$ bond distance average (2.070 and 2.047 Å for **2** and its analogue, respectively) is comparable, while the $Cu–N^{NCS}$

distance of the analogue (2.596 Å) is much longer than in **1** (2.129 Å, an average of the two independent units), showing that the elongation in octahedral geometry is more significant than in square pyramidal geometry. Similarly, in **1**, a mean plane through the coordinated atoms of the ACE with copper(II) ion revealed that these atoms do not lie in a plane (r.m.s. deviation: 0.287 and 0.315 Å for N21 and N8 atoms) while in the octahedral analogue of **2** these atoms are lied on a plane with no negligible r.m.s. deviation.

Similarly in **1**, the average of the N–Cu–N bond angles in six-membered and five-membered chelate rings (93.33 and 84.85º, average of two independent units, respectively) are similar to the CSD average (93.86 and 85.50 º, respectively [13]). In a similar fashion to **1**, one of the 1,3-diazacyclohexane rings of ACE has a different conformation than its non-ionic analogue, showing that the ACE ligand is coordinated to the copper(II) ion in its rare isomeric form. **2** contains four chiral centers; two secondary amine groups have the same enantiomeric form which is different than that of the two tertiary ones. However the crystals contain a racemic mixture of *R*,*S*,*R*,*S* and *S*,*R*,*S*,*R* isomers. In the crystal structure of **2**, there is a strong hydrogen bonding network involving the N–H groups on the macrocycle ions, both the bound and free thiocyanato anions, and the water and methanol solvent molecules (Table 3).

3.2.3. Crystal structure of [Cu(ACE)(μ-N_3)]$_n$[N_3]$_n$ (3)

X-ray analysis of **3** revealed a 1D coordination polymer of macrocyclic copper(II), bridged by azido ligands forming a zigzag chain propagating down the *a* axis [32, 64]. In the crystal structure of **3** (Fig. 4), the copper(II) ion is in an elongated octahedral coordination environment, in which the four donor nitrogen atoms of the ACE macrocycle are located in the equatorial positions with an average Cu–N bond lengths of 2.054 Å which is comparable to the CSD

average (2.013 Å [13]). The axial sites are occupied by terminal nitrogen atoms of the two azido ligands. The axial bond length average (2.498 Å) is much longer than those of the equatorial ones due to Jahn-Teller effects. The mean plane through the coordinated atoms of ACE with copper(II) ion shows negligible deviation from the plane. In this structure, the ACE ligand adopts its more common isomeric form. The average of the N–Cu–N bond angles in six-membered and five-membered chelate rings (93.12 and 86.88º) are similar to the CSD average and although the structure is contains four chiral centers, the crystals contain a racemic mixture of *R*,*S*,*R*,*S* and *S*,*R*,*S*,*R* isomers.

3.2.4. Docking studies

For predicting the biological activities of the ACE and ACD ligands, along with complexes **1** and **2**, interactions of these compounds with ten macromolecular receptors were studied using Gold [49] docking software. In addition to these compounds, the non-ionic analogues of **1** and **2** were added to the docking list. The Gold docking results are reported in terms of the values of fitness, with higher fitness indicating a better docking interaction [32-35, 62]. The results of the docking studies presented in this work are the best binding results out of the ten favorites predicted by Gold. Also for evaluation of the calculated fitness values, these scores were compared with those of the famous anti-cancer drug, doxorubicin (a cancer medication that interferes with the growth and spread of cancer cells in the body [65, 66]).

The general features from the Gold docking prediction (Table 4) show that all studied structures can be considered as biologically active compounds [32-34, 62]. The best predicted protein target for two of the macrocyclic ligands is HDAC7. Based on the calculated fitness values, the ACE ligand can interact with studied proteins better than the ACD, showing that the

1,3-diazacyclohexane rings increases the binding ability of the ACE. Also this study revealed that **2** can interact better than the free ligand (ACE) and also complex **1** (except for HDAC7) which can be attributed to the thiocyanato ligand effect. A similar result has been observed for the cytotoxic effect of two similar copper complexes containing different halido ligands [34]. Table 4 reveals that the structures of **1** and **2** in many cases have higher scores than their non-ionic forms. Also these compounds can bind in the minor grooves of DNA (Figures 5 and 6), which makes these compounds a good choice for DNA binding studies. Among the studied compounds, the DNA-binding ability of the ACD was higher than the others with the order of **2** > ACD > ACE > analogue **2** > **1** > analogue **1**. The calculations revealed that the studied compounds have higher or comparable fitness scores to doxorubicin in docking toward Top II (**2**), DNA-Gyrase (**2**, analogue **2**) and CatB (**2**, analogue **2**) proteins.

4. Conclusion

The 1,3,6,10,12,15-hexaazatricyclo[13.3.1.$1^{6,10}$]eicosane complexes of copper(II) ion, $[Cu(ACE)NO_3]NO_3$ (**1**), [Cu(ACE)NCS]NCS (**2**), $[Cu(ACE)(\mu\text{-}N_3)]_n[N_3]_n$ (**3**), were prepared by template synthesis, followed by ion exchange reactions and their spectral and structural properties were investigated. Complex **1** is an intermediate product which can be formed during the ion exchange reaction of its non-ionic $[Cu(ACE)(NO_3)_2]$ compound and could be an evidence for SN1 mechanism of ion exchange reactions on its non-ionic parent molecule. In the structures of **1** and **2**, the copper(II) ion has a distorted square pyramidal geometry with CuN_5 environment. The geometry of the copper(II) ion in the 1D-coordination polymer of **3** is octahedral, where bridging azido ligands extend the polymer down the *a* axis. All complexes have Jahn-Teller distortion; the N_4-donor ACE ligand lies on the equatorial plane, with axial positions being filled by the other ligands. Docking studies revealed that the ACE ligand and its complexes **1** and **2** can

interact with biomacromolecules (BRAF kinase, CatB, DNA gyrase, HDAC7, rHA, RNR, TrxR, TS and Top II), with the best predicted target for ACE being HDAC7, Top II for **1** and **2**. Since these compounds can place in the minor grooves of the DNA molecule, studying anticancer activities of these compounds could be interesting.

Appendix A. Supplementary data

CCDC 1873477−1873479 for complexes **1**−**3**, respectively, contain the supplementary crystallographic data for this paper. These data can be obtained free of charge *via* www.ccdc.cam.ac.uk/conts/retrieving.html [or from the Cambridge Crystallographic Data Centre (CCDC), 12 Union Road, Cambridge CB21EZ, UK; fax: +44(0)1223-336033; email: deposit@ccdc.cam.ac.uk]. Structure factor table is available from the authors.

References

[1] D. K. Cabbiness, D. W. Margerum, *J. Am. Chem. Soc.*, **91**, 6540 (1969).

[2] L. F. Lindoy, *The Chemistry of Macrocyclic Ligand Complexes*, Cambridge: Cambridge University Press, UK, (1989).

[3] R. D. Hancock, *J. Chem. Educ.*, **69**, 615 (1992).

[4] D. E. Fenton, *Chem. Soc. Rev.*, **28**, 159 (1999).

[5] *Coordination chemistry of macrocyclic compounds*, Springer US, Plenum Press, New York, (1979).

[6] D. Parker, *Chem. Soc. Rev.*, **33**, 156 (2004).

[7] D. Parker, *Coord. Chem. Rev.*, **205**, 109 (2000).

[8] M. K. Beklemishev, S. Elshani, C. M. Wai, *Anal. Chem.*, **66**, 3521 (1994).

[9] Q. Cheng, Y. Wan, L. Wang, G. Liao, Z. Pan, *Polyhedron*, 249 (2018).

[10] Y. Chen, H. Song, J. Mao, M. Liu, C. Ding, Z. Pan, *Inorg. Chem. Commun.*, **27**, 131 (2013).

[11] S. Gu, J. Huang, X. Liu, H. Liu, Y. Zhou, W. Xu, *Inorg. Chem. Commun.*, **21**, 168 (2012).

[12] B. P. Burke, S. J. Archibald, *Annu. Rep. Prog. Chem., Sect. A: Inorg. Chem.*, **109**, 232 (2013).

[13] M. Hakimi, Z. Mardani, K. Moeini, F. Mohr, *Z. Naturforsch.*, **72b**, 115 (2017).

[14] M. Hakimi, K. Moeini, Z. Mardani, F. Mohr, *Polyhedron*, **70**, 92 (2014).

[15] M. Hakimi, K. Moeini, Z. Mardani, M. A. Fernandes, F. Mohr, E. Schuh, *J. Coord. Chem.*, **65**, 1232 (2012).

[16] S. R. Collinson, D. E. Fenton, *Coord. Chem. Rev.*, **148**, 19 (1996).

[17] D. E. Fenton, H. Okawa, *J. Chem. Soc., Dalton Trans.*, 1349 (1993).

[18] D. Schols, S. Struyf, J. V. Damme, J. A. Esté, G. Henson, E. D. Clercq, *J. Exp. Med.*, **186**, 1383 (1997).

[19] A. Chaudhary, N. Bansal, A. Gajraj, R. V. Singh, *J. Inorg. Biochem.*, **96**, 393 (2003).

[20] P. Gull, M. A. Malik, O. A. Dar, A. A. Hashmi, *Microb. Pathog.*, **104**, 212 (2017).

[21] A. Dees, A. Zahl, R. Puchta, N. J. R. Van Eikema Hommes, F. W. Heinemann, I. Ivanović-Burmazović, *Inorg. Chem.*, **46**, 2459 (2007).
[22] C. Liu, J. Zhou, Q. Li, L. Wang, Z. Liao, H. Xu, *J. Inorg. Biochem.*, **75**, 233 (1999).
[23] D. K. Chand, H.-J. Schneider, J. A. Aguilar, F. Escartí, E. García-España, S. V. Luis, *Inorg. Chim. Acta*, **316**, 71 (2001).
[24] N. Shahabadi, M. Hakimi, T. Morovati, S. Hadidi, K. Moeini, *Lumin.*, **32**, 43 (2017).
[25] N. Shahabadi, M. Hakimi, T. Morovati, N. Fatahi, *Nucleos. Nucleot. Nucl.*, **36**, 497 (2017).
[26] Z. P. Li, B. H. Liu, *J. Appl. Electrochem.*, **40**, 475 (2010).
[27] J. H. Zagal, S. Griveau, J. F. Silva, T. Nyokong, F. Bedioui, *Coord. Chem. Rev.*, **254**, 2755 (2010).
[28] K. Tammeveski, J. H. Zagal, *Curr. Opin. Electrochem.*, **9**, 207 (2018).
[29] B. Ghanbari, L. Shahhoseini, H. Hosseini, M. Bagherzadeh, A. Owczarzak, M. Kubicki, *J. Organomet. Chem.*, **866**, 72 (2018).
[30] L.-M. Zhang, H.-Y. Li, H.-X. Li, D. J. Young, Y. Wang, J.-P. Lang, *Inorg. Chem.*, **56**, 11230 (2017).
[31] J. Gao, F. R. Woolley, R. A. Zingaro, *Org. Biomol. Chem.*, **3**, 2126 (2005).
[32] F. Marandi, K. Moeini, F. Alizadeh, Z. Mardani, C. K. Quah, W.-S. Loh, J. D. Woollins, *Inorg. Chim. Acta*, **482**, 717 (2018).
[33] F. Marandi, K. Moeini, F. Alizadeh, Z. Mardani, C. K. Quah, W.-S. Loh, *Z. Naturforsch.*, **73b**, 369 (2018).
[34] Z. Mardani, R. Kazemshoar-Duzduzani, K. Moeini, A. Hajabbas-Farshchi, C. Carpenter-Warren, A. M. Z. Slawin, J. D. Woollins, *RSC Adv.*, **8**, 28810 (2018).
[35] A. A. Adeniyi, P. A. Ajibade, *Molecules*, **18**, 3760 (2013).
[36] N. H. Moghadam, S. Salehzadeh, N. Shahabadi, *Nucleos. Nucleot. Nucl.*, **36**, 553 (2017).
[37] F. Marandi, K. Moeini, B. Mostafazadeh, H. Krautscheid, *Polyhedron*, **133**, 146 (2017).
[38] A. L. Fuller, L. a. S. Scott-Hayward, Y. Li, M. Bühl, A. M. Z. Slawin, J. D. Woollins, *J. Am. Chem. Soc.*, **132**, 5799 (2010).
[39] *CrystalClear-SM Expert v3.1b27. Rigaku Americas, The Woodlands, Texas, USA, and Rigaku Corporation, Tokyo, Japan*, in, (2013).
[40] *CrysAlisPro v1.171.38.41. Rigaku Oxford Diffraction, Rigaku Corporation, Oxford, U.K.*, in, (2015).
[41] G. Sheldrick, *Acta Crystallogr.*, **A71**, 3 (2015).
[42] G. Sheldrick, *Acta Crystallogr.*, **C71**, 3 (2015).
[43] O. V. Dolomanov, L. J. Bourhis, R. J. Gildea, J. a. K. Howard, H. Puschmann, *J. Appl. Crystallogr.*, **42**, 339 (2009).
[44] A. Spek, *Acta Crystallogr.*, **C71**, 9 (2015).
[45] L. J. Farrugia, *J. Appl. Crystallogr.*, **30**, 565 (1997).
[46] M. N. Burnett, C. K. Johnson, Ortep-III, Report ORNL-6895. Oak Ridge National Laboratory, Oak Ridge, Tennessee, U.S., (1996).
[47] G. Bergerhof, M. Berndt, K. Brandenburg, *J. Res. Natl. Stand. Technol.*, **101**, 221 (1996).
[48] A. Gavezzotti, *Acc. Chem. Res.*, **27**, 309 (1994).
[49] G. Jones, P. Willett, R. C. Glen, A. R. Leach, R. Taylor, *J. Mol. Biol.*, **267**, 727 (1997).
[50] M. Hakimi, K. Moeini, Z. Mardani, E. Schuh, F. Mohr, *J. Coord. Chem.*, **66**, 1129 (2013).
[51] M. Hakimi, Z. Mardani, K. Moeini, *J. Korean Chem. Soc.*, **57**, 447 (2013).

[52] M. Hakimi, Z. Mardani, K. Moeini, E. Schuh, F. Mohr, *Z. Naturforsch.*, **68b**, 267 (2013).
[53] M. Hakimi, K. Moeini, Z. Mardani, F. Khorrami, *J. Korean Chem. Soc.*, **57**, 352 (2013).
[54] K. Nakamoto, 6 (Ed.) Infrared and raman spectra of inorganic and coordination compounds, John Wiley, Hoboken, (2009), pp. 285.
[55] F. H. Allen, *Acta Crystallogr.*, **B58**, 380–388 (2002).
[56] M. Hakimi, Z. Mardani, K. Moeini, F. Mohr, *Synthesis and characterization of a macrocyclic copper complex containing the 14-membered 1,3,5,8,10,12-hexaazacyclotetradecane unit*, in: Z. Naturforsch., (2017), pp. 115.
[57] X. Jiang, H.-Z. Kou, *Chem. Commun.*, **52**, 2952 (2016).
[58] X. Jiang, K.-Q. Hu, H.-Z. Kou, *CrystEngComm*, **18**, 4084 (2016).
[59] R. W. Hay, A. Danby, P. Lightfoot, *Transit. Met. Chem.*, **22**, 395 (1997).
[60] A. W. Addison, T. Rao, J. Reedjik, J. V. Rijn, G. Verschoor, *J. Chem. Soc., Dalton Trans.*, 1349 (1984).
[61] M. Hakimi, Z. Mardani, K. Moeini, F. Mohr, *Polyhedron*, **102**, 569 (2015).
[62] Z. Mardani, V. Golsanamlou, Z. Jabbarzadeh, K. Moeini, S. Khodavandegar, C. Carpenter-Warren, A. M. Z. Slawin, J. D. Woollins, *J. Coord. Chem.*, Accepted (2018).
[63] J. Perlstein, *J. Am. Chem. Soc.*, **123**, 191 (2001).
[64] L. Saghatforoush, K. Moeini, V. Golsanamlou, V. Amani, A. Bakhtiari, Z. Mardani, *Inorg. Chim. Acta*, **483**, 392 (2018).
[65] https://www.drugs.com/mtm/doxorubicin.html, in, (7/19/2018).
[66] F. Marandi, K. Moeini, A. Arkak, Z. Mardani, H. Krautscheid, *J. Coord. Chem.*, Accepted (2018).

Table 1. Crystal data and structure refinement for complexes **1**–**3**.

	1	**2**	**3**
Empirical formula	$C_{14}H_{30}CuN_7O_3 \cdot NO_3$	$4[C_{15}H_{28}CuN_7S]^{+} \cdot 4[CNS]^{-} \cdot 2(H_2O)$ CH_4O	$C_{14}H_{30}CuN_9$ $[N_3]^{-}$
Formula weight, g mol^{-1}	470.00	1916.63	430.04
Crystal size, mm^3	0.36 × 0.27 × 0.15	0.12 × 0.02 × 0.02	0.10 × 0.06 × 0.03
Temperature, K	125	173	93
Crystal system	Orthorhombic	Monoclinic	Monoclinic
Space group	*Pbca*	$P2_1/n$	$P2_1/n$
Unit cell dimensions			
a, Å	22.062(5)	8.88158(15)	6.8191(2)
b, Å	16.332(4)	48.2663(7)	12.8245(4)
c, Å	10.955(2)	10.25700(17)	11.5862(4)
β, °	90	94.163(2)	95.849(3)
Volume, $Å^3$	3947.3(15)	4385.38(12)	1007.96(6)
Z	8	2	2

Calculated density, g cm^{-3}	1.582	1.446	1.417
Absorption coefficient, mm^{-1}	1.158	1.210	1.751
$F(000)$, e	1976	2020	454
θ range for data collection, °	2.2–28.7	1.7–28.3	3.4–74.4
h, k, l ranges	$-29 \le h \le 28$, $-21 \le k \le 22$, $-14 \le l \le 14$	$-11 \le h \le 11$, $-63 \le k \le 63$, $-13 \le l \le 13$	$-8 \le h \le 8$, $-16 \le k \le 15$, $-14 \le l \le 14$
Reflections collected / independent / R_{int}	53214 / 4928 / 0.082	150109 / 10027 / 0.082	11305 / 2046 / 0.074
Data / restraints / parameters	4928 / 2 / 270	10027 / 10 / 546	2046 / 1 / 117
Goodness-of-fit on F^2	1.03	1.21	1.11
$R1$ / $wR2$ ($I \ge 2\ \sigma(I)$)	0.0366 / 0.0960	0.0659/ 0.1268	0.0480/ 0.1351
$R1$ / $wR2$ (all data)	0.0569 / 0.1031	0.0956/ 0.1327	0.0493/ 0.1360
Largest diff. peak / hole, e $Å^{-3}$	0.50 / −0.30	0.73 / −0.87	0.74 / −0.58

Table 2. Selected bond length (Å) and angles (°) for complexes **1**−**3** with estimated standard deviations in parentheses.

	Bond lengths (Å)		Bond Angles (°)	
Complex **1**	Cu1–N1	2.0152(18)	N1–Cu1–N5	93.34(7)
	Cu1–N5	2.0928(17)	N1–Cu1–N8	177.29(7)
	Cu1–N8	2.0069(16)	N1–Cu1–N12	85.85(7)
	Cu1–N12	2.0684(16)	N1–Cu1–O15	80.23(6)
	Cu1–O15	2.2947(15)	N16–O15– Cu1	124.26(12)
Complex **2**	Cu1–N1	2.070(4)	N1–Cu1–N5	92.93(15)
	Cu1–N5	2.083(4)	N1–Cu1–N8	145.10(16)
	Cu1–N8	2.040(4)	N1–Cu1–N12	84.92(15)
	Cu1–N12	2.095(4)	N1–Cu1–N15	97.74(17)
	Cu1–O15	2.115(4)	C15–N15– Cu1	153.3(4)
	Cu21–N21	2.044(4)	N21–Cu21–N25	93.50(14)
	Cu21–N25	2.098(4)	N21–Cu21–N28	148.56(15)
	Cu21–N28	2.043(3)	N21–Cu21–N32	85.03(14)

		Cu21–N32	2.084(3)	N21–Cu21–N35	104.49(16)
		Cu21–O35	2.143(4)	C35–N35– Cu21	160.8(4)
Complex	**3**	Cu1–N1	1.997(2)	N1–Cu1–N1^{i}	180.00(15)
		Cu1–N5	2.111(2)	N1–Cu1–N5	93.16(8)
		Cu1–N6	2.498(3)	N1–Cu1–N5^{i}	86.84(8)

Table 3. Hydrogen bonds and short contacts dimensions (Å and °) in complexes **1** and **2**.

	D–H···A	*d*(D–H)	*d*(H···A)	<(DHA)	*d*(D···A)
1	N(1)–H(1)···O(19)	0.960(9)	2.218(13)	150.9(16)	3.092(3)
	N(8)–H(8)···O(17)^{i}	0.957(9)	2.188(14)	142.7(15)	3.006(2)
2	N(1)–H(1)···S(35)	0.946(19)	2.52(3)	150(4)	3.372(4)
	N(8)–H(8)···S(15)^{ii}	0.941(19)	2.49(3)	155(4)	3.363(4)
	N(21)–H(21) ···N(42)	0.945(19)	2.29(3)	142(4)	3.088(7)
	N(28)–H(28) ···S(41)	0.943(19)	2.48(2)	158(4)	3.369(4)
	O(43)–H(43D) ···S(35)	0.960(5)	2.344(10)	175(5)	3.301(5)
	O(43)–H(43E) ···N(42)	0.961(5)	1.850(12)	174(6)	2.807(9)
	O(44)–H(44) ···O(43)	0.84	1.97	155	2.751(11)

Symmetry Operators: i) 1-x, 1-y, 1-z ii) 2-x,1-y,-z

Table 4. The calculated fitness values for ACD and ACE ligands, complexes **1** and **2** and their analogues along with the doxorubicin.

	B-DNAs/Min	BRAF-Kinase	CatB	DNA-Gyrase	HDAC7	rHA	RNR	TrxR	TS	Top II
ACD	46.57	33.24	16.42	32.59	42.38	23.69	31.07	34.67	32.50	32.23
ACE	39.92	39.20	21.26	37.35	46.17	35.15	39.33	42.36	36.16	39.59
Complex **1**	32.13	40.95	21.08	45.04	31.67	43.70	40.11	38.96	36.91	46.54
Analogue of **1**	28.21	11.51	18.95	44.18	−24.23	30.86	36.85	26.76	41.23	42.02
Complex **2**	51.35	44.39	24.42	49.91	37.09	46.80	42.70	50.38	43.99	57.02
Analogue of **2**	38.90	37.60	27.27	55.16	35.35	43.82	42.61	37.33	48.65	52.59
Doxorubicin	83.10	54.21	25.95	52.97	50.73	50.10	49.18	66.70	53.34	59.05

Figure Captions

Scheme 1. The structure of 1,3,6,10,12,15-hexaazatricyclo[13.3.1.1^{6,10}]eicosane (ACE) and 1,3,5,8,10,12-hexaazacyclotetradecane (ACD).

Figure 1. Pie chart; percentage of different metals coordinated toward ACD unit.

Figure 2. An ORTEP plot of the asymmetric unit of **1**, showing thermal ellipsoids at 50% probability, the heteroatom labelling scheme and some of the inter/intramolecular hydrogen bonding present.

Figure 3. An ORTEP plot of the asymmetric unit of **2**, showing thermal ellipsoids at 50% probability, the heteroatom labelling scheme and some of the inter/intramolecular

hydrogen bonding present. The asymmetric unit contains two molecules of the compound, two free thiocyanato counterions, a full occupancy water of solvation and a half occupancy methanol, disordered over an inversion center.

Figure 4. An ORTEP plot of one copper macrocyclic unit of **3**, with the azido bridge either side, showing thermal ellipsoids at 50% probability, along with the heteroatom labelling scheme.

Figure 5. Docking study results, showing the interaction between the complex **1** and B-DNA (minor groove).

Figure 6. Docking study results, showing the interaction between the complex **2** and B-DNA (minor groove).

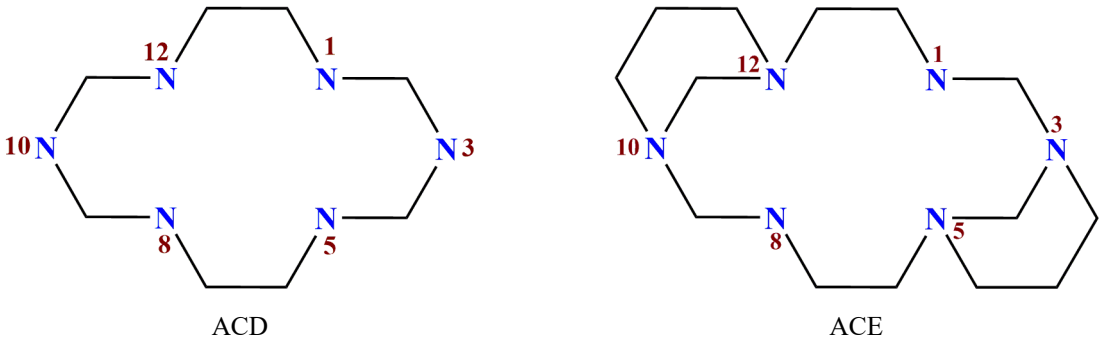

Scheme 1.

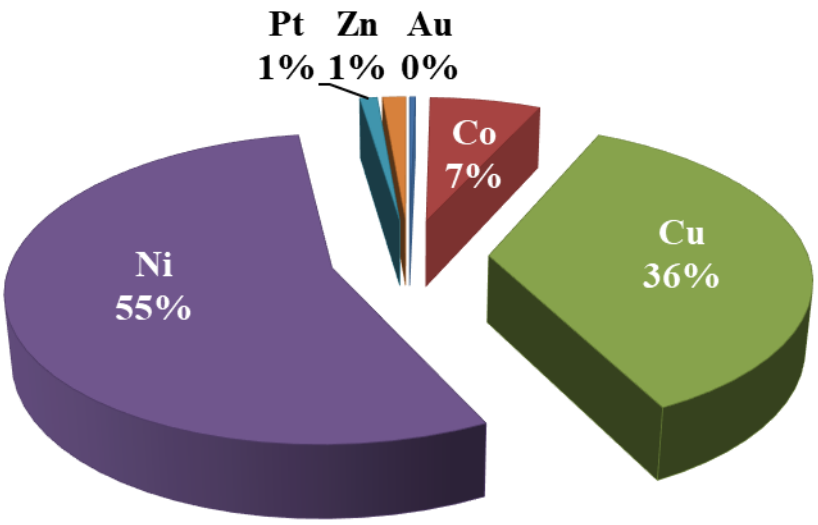

Figure 1.

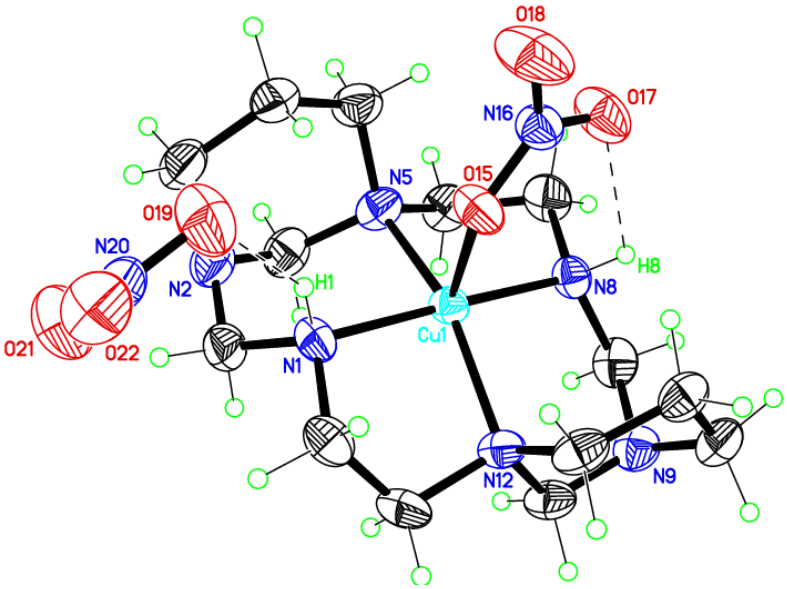

Figure 2.

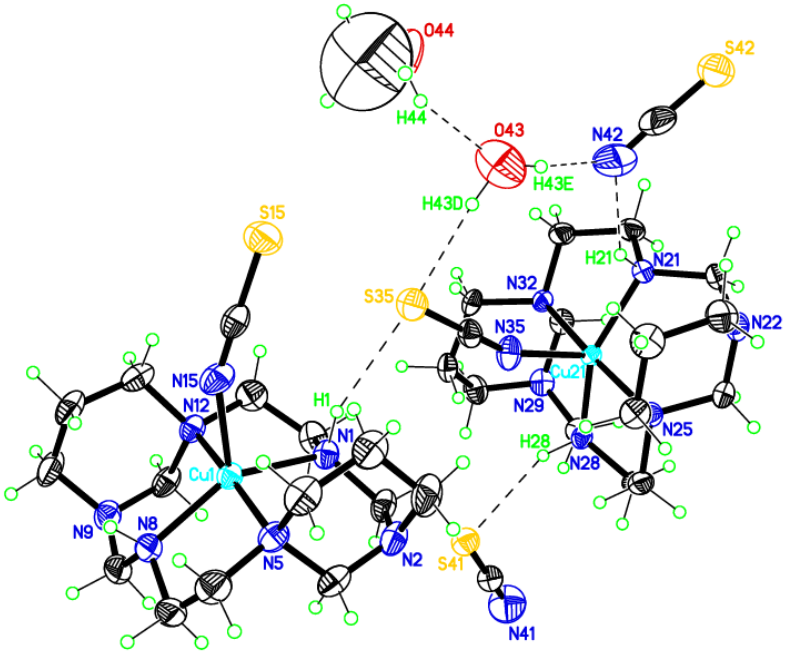

Figure 3.

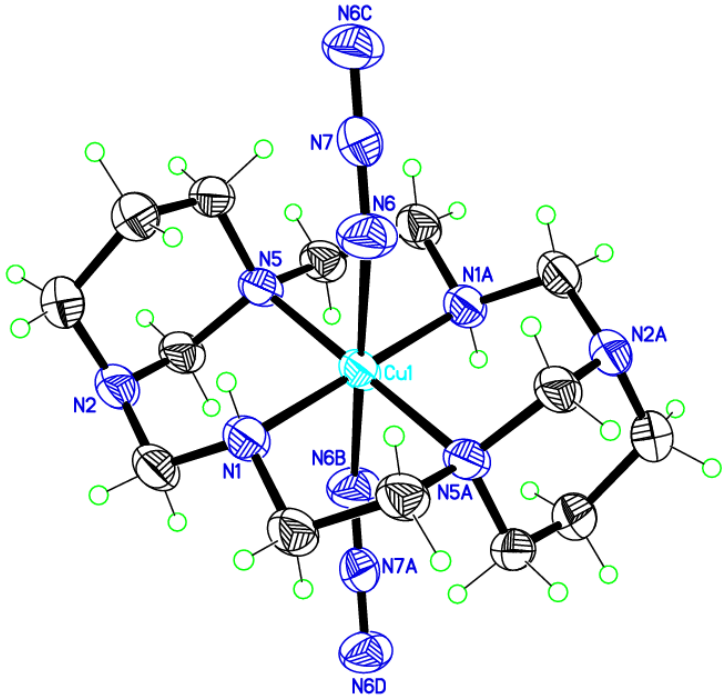

Figure 4.

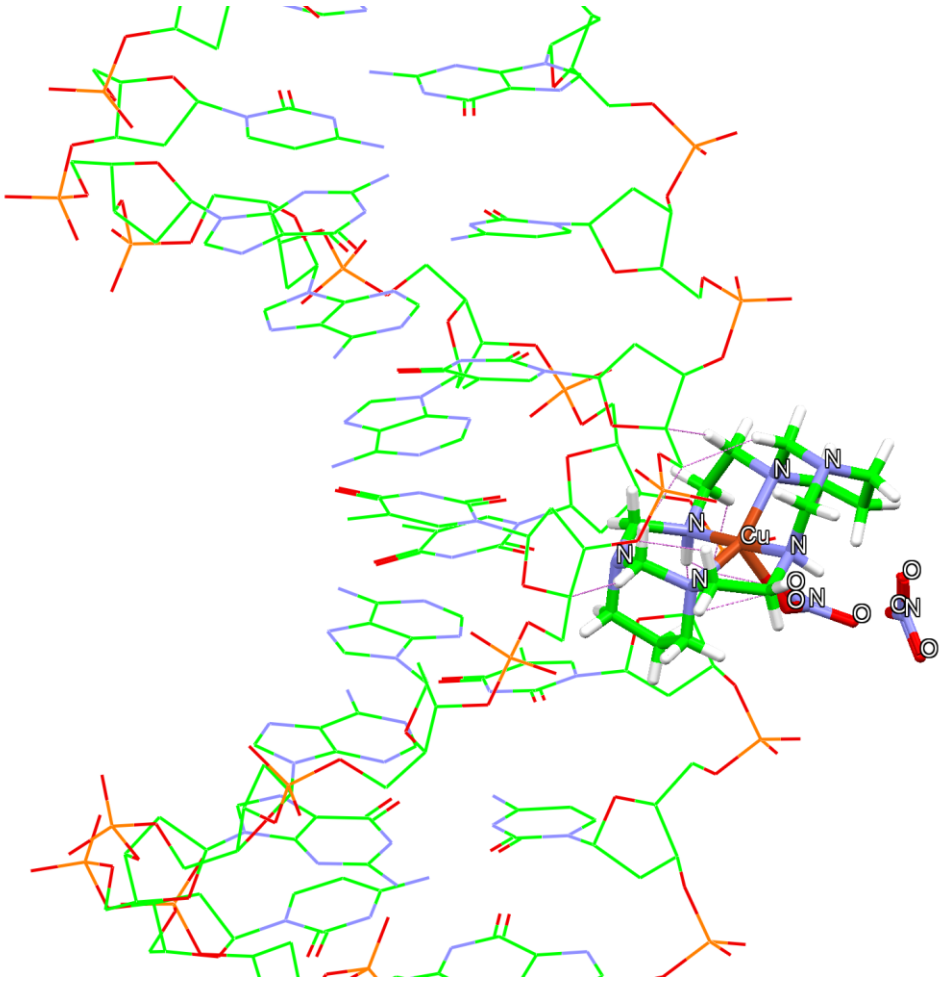

Figure 5.

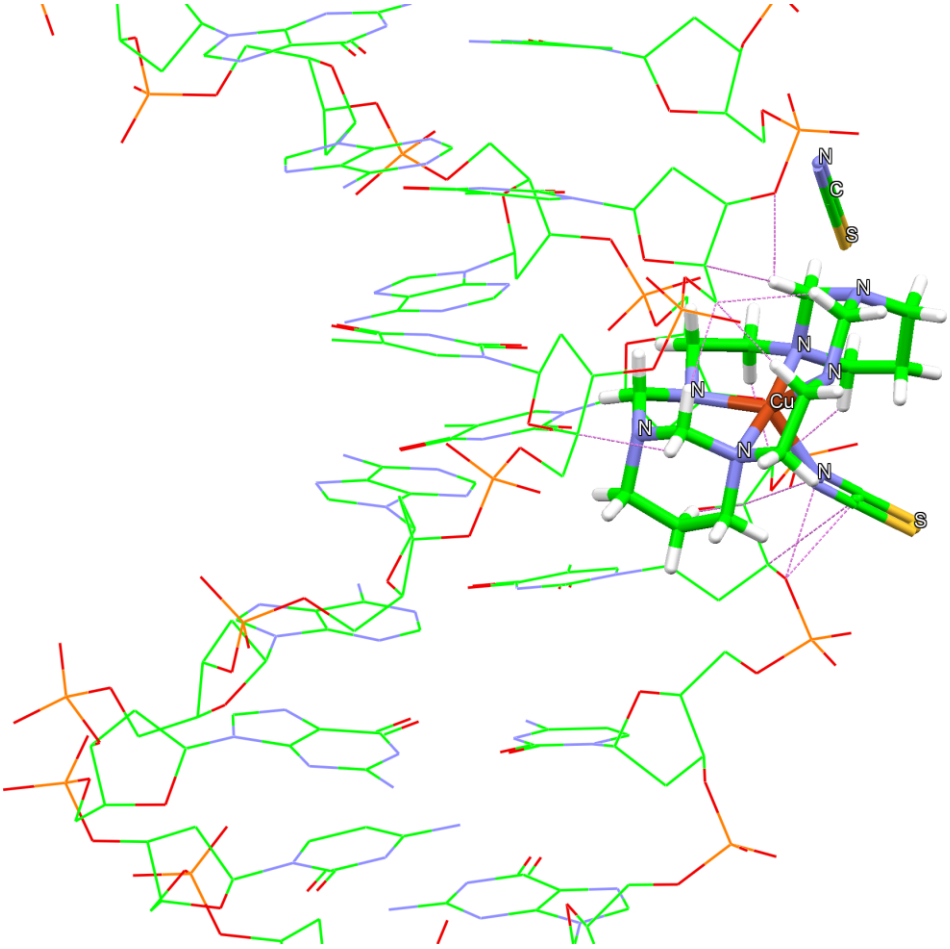

Figure 6.